ANALYSIS OF FAILURE AND DEGRADATION MODES OF SMALL-SCALE PHOTOVOLTAIC POWER PLANTS IN RURAL COMMUNITIES OF THE ATACAMA DESERT

Pía Vásquez[1], Rodrigo Palma-Behnke[1,2], Ignacia Devoto[1,2]

[1] Department of Electrical Engineering, University of Chile
[2] Energy Center, University of Chile, Chile

Abstract

In this work, a detailed analysis is performed on failure/degradation modes identified in 95 solar photovoltaic modules located in small-scale domestic PV power plants operating in the Atacama Desert, Chile. The data used was collected in a previous work via visual inspection, thermal imaging and electrical characterization of the I-V curve. Additionally, in-field data is complemented with the global trends identified in the sample universe, together with a theoretical analysis about the possible failure/degradation mechanisms involved. As a result, eight different anomalies were identified and described: soiling, hotspots, delamination, front cover glass discoloration, partial shading, cell fracture, faulty soldering and PID. The most common anomalies were soiling and hotspots, being the highest cell temperature around 100°C. With this information, possible failure/degradation mechanisms were inferred, as well as the influence of the local environment on module components, which may be involved in degradation and the occurrence of failures. This work constitutes a first effort to characterize small-scale domestic PV solutions in extreme Chilean desert conditions.

Keywords: PV modules, failure/degradation modes and mechanisms.

1. Introduction

Technological improvements in solar photovoltaic (SPV) devices require the analysis of their actual in-field performance during complete lifetime. In the present time, manufacturers and researchers evaluate the behavior of SPV modules under different climatic conditions and external stress by means of accelerated tests (AT) (Sai Tatapudi, 2018). However, these AT techniques involve applying external stress variables (UV radiation, soiling, humidity, thermal cycles, damp heat exposure, etc.) in levels higher than they occur under normal operating conditions to induce failure/degradation modes quickly (Eder, et al., 2018). Although this can be effective to determine whether a failure/degradation mode can occur to the SPV module under certain external conditions, information related to the time of exposure until the equipment fail may be less reliable (Subramaniyan, et al., 2018). In this scenario, in-field gathered information regarding to real time operation of modules can help to complement AT results and even contribute to improve testing techniques (Felder, et al., 2015). An important issue is that, obviously, SPV modules manufacturers are located in specific climatic conditions, thus, information of in-field modules from other locations can be difficult or impossible to acquire. In this work, data from 95 in-field modules operating in the Atacama Desert (northern zone of Chile) were analyzed, to identify failures and degradation modes shown by small-scale SPV power plants subjected to the dry-arid climatic conditions, characteristic of this location. The main interest in this region is due to the high irradiation conditions (both GHI and DNI) and clear skies through the year, which can ensure a constant and efficient solar electricity production and supply (Rondanelli, et al., 2015). With this in mind, and combined with the well settled hydraulic generation coming from the southern regions of the country, the Chilean government has set into the country energy strategy the goal of 70% of electricity generation from renewable sources by 2050 (Energía, 2014). Additionally, recent R&D&I initiatives have proposed the local development of SPV modules specifically adapted to Atacama Desert climate (Ferrada, et al., 2015). However, the high availability of solar resource includes both UV-A and UV-B radiation, which have been found to be detrimental to SPV modules performance in the long term (Trang, et al., 2016). However, degradation of modules over time occurs as a consequence of many external and internal features (manufacturing processes, material quality, installation procedures, transport and storage, among others) interacting together and causing subsequent degradation or even failure. In (Jordan, et al., 2017), degradation rates of electrical parameters (short circuit current, open circuit voltage, maximum power point) of SPV modules around the world show that the highest degradation occurs for modules located in hot and humid places, while in hot and dry climate the degradation is less pronounced.

In the previous research (Devoto, 2018), the modules analyzed in this work were systematically surveyed by means of an IDCTool (Inspection Data Collection Tool) developed and tested for the desert climatic conditions

© 2019. The Authors. Published by International Solar Energy Society
Selection and/or peer review under responsibility of Scientific Committee
doi:10.18086/swc.2019.52.02 Available at http://proceedings.ises.org

of the Atacama Desert. The degradation rates, calculated in the previous work, show results in accordance with worldwide research (Angèle, et al., 2016). Higher drops in short circuit current (I_{sc}) than in open circuit voltages (V_{oc}) determine the total P_{mpp} degradation rates, which is probably related to the predominant presence of soiling phenomena, characteristic of dusty environments as deserts.
Regarding to visual degradation and failures, a literature review reports that the most common anomalies in desert climates are encapsulant discoloration and backsheet insulation loss. Most failures affect modules after ten years of operation (Jordan, et al., 2017), in particular for modules deployed prior 2000. Other anomalies like internal circuitry (IC) discoloration/failure, delamination, backsheet insulation loss and hotspots are also documented but to a lesser extent (Jordan, et al., 2017). Moreover, data show that while modules deployed post 2000 show notably less failures (in %) than those deployed prior 2000, the number of affected modules is not excessively lower. Again, for desert climate the failures occurrence is notably less than for hot and humid conditions, and even moderate climate conditions. The results reported in the previous work show that, apart from soiling, modules operating in the dry and arid Atacama Desert appear to be affected by hotspots, localized EVA encapsulant delamination, front glass discoloration, among others (Devoto, 2018). As any other desert location, soiling is the most common environmental issue that visually affects panels. Soiling produces different effects as abrasion, optical efficiency and energy yield losses or temperature differences across the module's surfaces, which contributes to accelerated degradation over time. As found in (Douglas, et al., 2017), the particles size that affect soiled modules is less than 63 µm diameter for modules installed in Atacama Desert. Particle size and elemental composition are influenced by natural environmental conditions but also by mining, agricultural facilities or cities nearby. Particles size can have different residence times over modules surfaces (Mazumder, et al., Photovoltaic Specialist Conference (PVSC)), ranging from hours (for coarse grains >3 µm diameter) to days or weeks for smaller particles. Their elemental composition may play a role in optical degradation of modules component materials through corrosion or weathering phenomena (Guiheneuf, et al., 2016), which (despite extreme aridity) is also observed in Atacama Desert PV rural power plants. The problems derived by soiling deposition can be highlighted for small-scale domestic or rural PV power plants, because they normally lack cleaning protocols and schedules. Additionally, the scarcity of water in the Atacama Desert carries higher cleaning costs that can be difficult to assume for small PV owners, who may prioritize water usage for agricultural purposes. In one hand, data recorded from this kind of installation allow to derive conclusions considering raw environmental (or human induced) conditions. On the other hand, information about installation conditions and periodicity of cleaning (or even whether the modules have been cleaned or not since their deployment) are important to evaluate possible causes of defects in SPV modules, which induce accelerated degradation or failures, and for this study this is not very clear.

This paper is organized as follows: In Section 2, methodology for the analysis is briefly explained, together with the description of the equipment and tools used. Furthermore, general features of the analyzed region and modules and criteria to detect and evaluate failure/degradation modes are presented. In Section 3, results are shown together with discussion of the possible failure/degradation mechanisms involved in the modes described. Finally, conclusions of this work are given in Section 4.

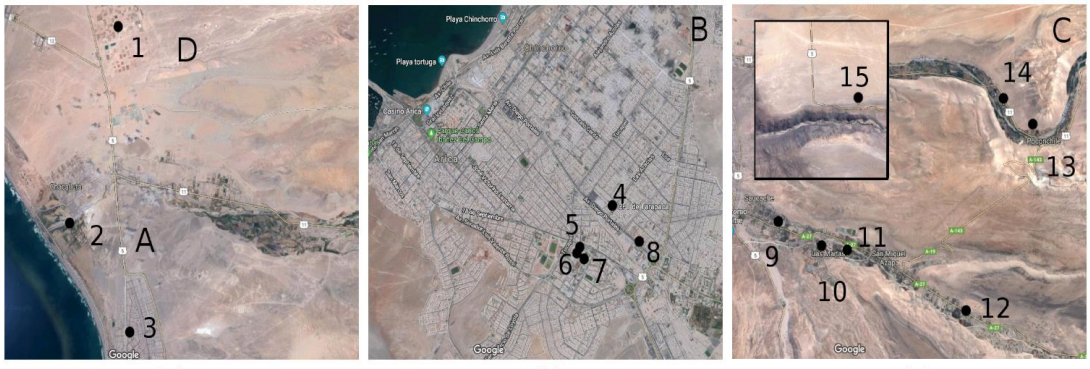

Fig. 1: Locations of 95 SPV modules evaluated in different zones of the Atacama Desert (a) coast, (b) city, (c) inner valley.

2. Methodology

For the analysis performed in this research, information about visual, electrical and thermal variables of SPV modules was used. Visual evaluation of modules was performed using a survey developed in the previous work by the authors (Devoto, 2018), thermal behavior was recorded using the IRT camera Flir One Pro. The images were filtered using MATLAB for better resolution. Electrical parameters (short circuit current I_{sc}, open circuit voltage V_{oc} and maximum power P_{mpp}) were recorded using an IV tracer from Seaward (PV210). The 95 evaluated SPV modules are located in four different zones of the Atacama Desert, which are shown in Figure 1:

Zone A (coast), zone B (city), zone C (inner valley) and zone D (inner coast). These zones are characterized by different environmental factors such as humidity coming from seashore, pollutants from the city, or higher presence of sand dust. The evaluation of three different parameters was performed using known behavior of electrical parameters and thermal patterns found in literature (Köntges, et al., 2014). Such behavior was related (when possible) with visual anomalies derived from visual inspection. The analysis is complemented with statistical treatment of the data, in order to identify trends of occurrence for failures/degradation, mainly for hotspots and soiled modules (the most extended anomalies in the sample universe). However, the small size of the sample does not assure statistical validity of the results. Additionally, general guidelines about the degradation/failure mechanisms are done, considering the analysis from a purely (theoretical) physical point of view. General data about the inspected modules is shown in Table 1.

Tab. 1: General information about investigated PV modules.

Manufacturer	Si Technology	Deployment year	Number of modules	% of total sample	Location
BP Solar	Multi-Si	-	1	1.05	6
Luxor	Multi-Si	2011	6	6.32	7
SolarWorld	Multi-Si	2012, 2013	30	31.58	2, 10-14
Risen Energy	Multi-Si	2013, 2015, 2016	24	25.26	1, 8
ET Towards Excellence	Multi-Si	2015	12	12.63	3, 4
JA Solar	Multi-Si	2015	3	3.16	7
SUNEL	Multi-Si	2012, 2016	9	9.47	9, 14
Hangwha Solar	Multi-Si	2012, 2015	4	4.21	1
Siemens	Mono-Si	2005	6	6.32	5, 15

From all the variety of failure/degradation modes that can be found in operating PV modules, attention was focused primarily in 14 anomalies detected in (Devoto, 2018). From these, additional selection was done considering those anomalies that could be analyzed using simultaneously at least two of the three types of inspected parameters (visual, thermal or electrical). With these criteria, eight different anomalies were analyzed: soiling, hotspots, delamination of EVA encapsulant, front glass milky discoloration, partial shading, cell fracture, faulty soldering and potential induced degradation (PID). A summary of the main features that allow to identify the anomalies is shown in Table 2, based in (Köntges, et al., 2014) and (Buerhop, et al., 2012).

Tab. 2: Identification of eight selected anomalies

Failure/degradation mode	Visual features	Electrical parameters	Thermal pattern
Soiling	Visible layer of dust	Reduction of Isc or also reduction in V_{oc} for severe soiling	-
Hotspots	-	Change in slope of the I-V characteristics near V_{oc} (flattening)	• Abnormal heating of one or more cells within a module, varying severity. • Abnormal temperature distribution within cell
Delamination of EVA	Loss of adhesion of EVA layers, localized or extended (bubble-like appearance)	-	Uneven temperature distribution in affected areas
Discoloration of front cover glass	Whitish appearance of front cover glass (localized or generalized)	-	Uneven temperature distribution in affected areas
Partial shading	Visible shadow projected by external object or localized drop	-	Uneven temperature distribution across shaded cells/modules
Cell fracture	-	Current mismatch	Uneven temperature distribution
Faulty soldering	Burn marks	Increased series resistance	Uneven temperature distribution
Potential induced degradation (PID)	-	• Reduction in V_{oc} • Rounding of the I-V curve knee	Lower cells warmer, close to frame

Although soiling is not a failure/degradation mode by itself, but a trigger of them or at least can be related to the appearance of anomalies, in this work is treated the same way as intrinsic failure/degradation of module

components. The analysis of soiling in (Devoto, 2018), differentiates the thickness of soiling layers. However, detailed inspection of features like distribution of soiling over the modules surface, intensity or deposition patterns was done additionally in this work. Furthermore, relationships between the presence of soiling layers and degradation of electrical parameters or thermal anomalies were also searched. Notice that all the analysis performed remains in a purely qualitatively plane, considering both the lack of well-defined standards to evaluate soiling rigorously (Menoufi, 2017) and the amount and detail of information available for this study. Also, well-defined definition of which amount of heating is considered as hotspot is not given. However, in this study, temperature differences of at least 10°C with respect to the module average temperature are considered as thermal anomalies. Since, both temperature differences between cells and within cells induce thermal stress in PV modules and can give rise to degradation and future failures, the two anomalies are considered as hotspots.

3. Results and Discussion

3.1. Soiling

Soiling was the most extended issue affecting the total sample universe. 89.5% of the inspected modules show soiling (either strong or light). Raw data show that, in accordance with literature, soiling layers contribute to reductions of the short circuit current more than open circuit voltage (which is affected mostly by temperature). However, these reductions can be significant as the thickness of the soiling layers increase. As the maximum power point depends directly on I_{sc} and V_{oc}, the power output of the module can be severely affected.

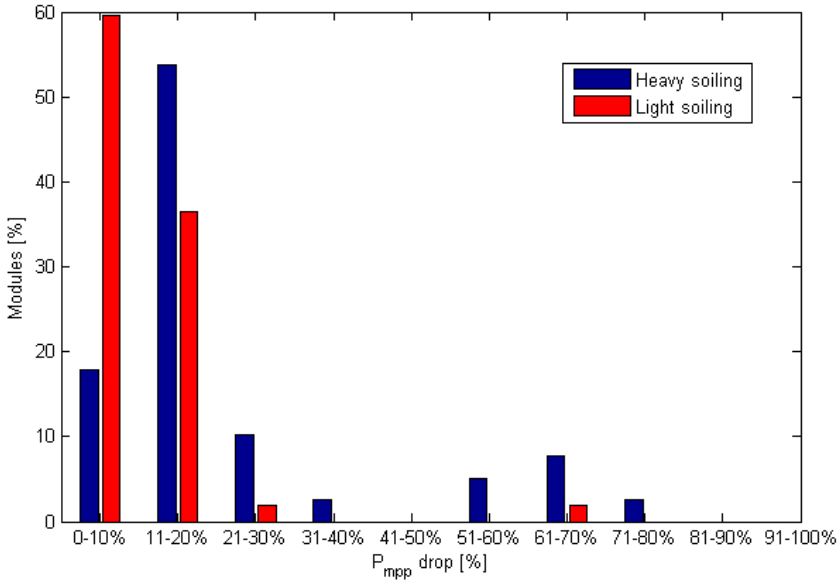

Fig. 2: Effects of degrees of soiling (light or heavy) on the maximum power point.

Moreover, depending on the distribution of soiling layers, additional thermal stress can be induced. From lightly soiled modules, it was found that 85% of them show I_{sc} reduction of less than 10% from the nominal value, while all of them show a reduction less than 20% from the nominal value. On the other hand, 80% of heavily soiled modules show I_{sc} drops up to 20%. However, 15% show I_{sc} drops higher than 40% from nominal value. Regarding to V_{oc}, both lightly and heavily soiled modules show drops less than 10% from the nominal value (except in two cases, for which higher V_{oc} drops can be attributable to other causes). The effect of the reductions of I_{sc} and V_{oc} on P_{mpp} is graphically shown in Figure 2, where P_{mpp} drop trends are dominated by I_{sc} rather than V_{oc}. As it will be seen later, heavily soiled modules show more varied P_{mpp} drops given that severity of soiling layers is more varied for heavily soiled modules than for lightly soiled modules.

For the case of heavily soiled modules, a detailed inspection of visual images shows that, apart from general information about the relationship of soiling with electrical parameters reduction, soiling deposition patterns can be distinguished according to the location of affected modules. As shown in Figure 3, for the four zones considered (see Figure 1), it was found that modules located near the seashore and outside the city (zone A and D) show a groove deposition pattern (type I), possibly related to humidity and wind (a). Inside the city, modules located near the seashore show inhomogeneous distribution of soiling layers (type II), attributable to the presence of pollutants from vehicles, industry or other activities inside the city (b). On the inner valley (c)

and (d), modules show a uniform distribution of soiling layers across the surface. Also, there was found a set of 6 modules with a particularly dense dust layer deposited on them, phenomena that was also reflected in the I-V measurements. For this reason, 'moderately' heavy soiled modules and 'extremely' heavy soiled modules are classified as type III and type IV respectively, considering that the difference between these two types is only the thickness of the soiling layer.

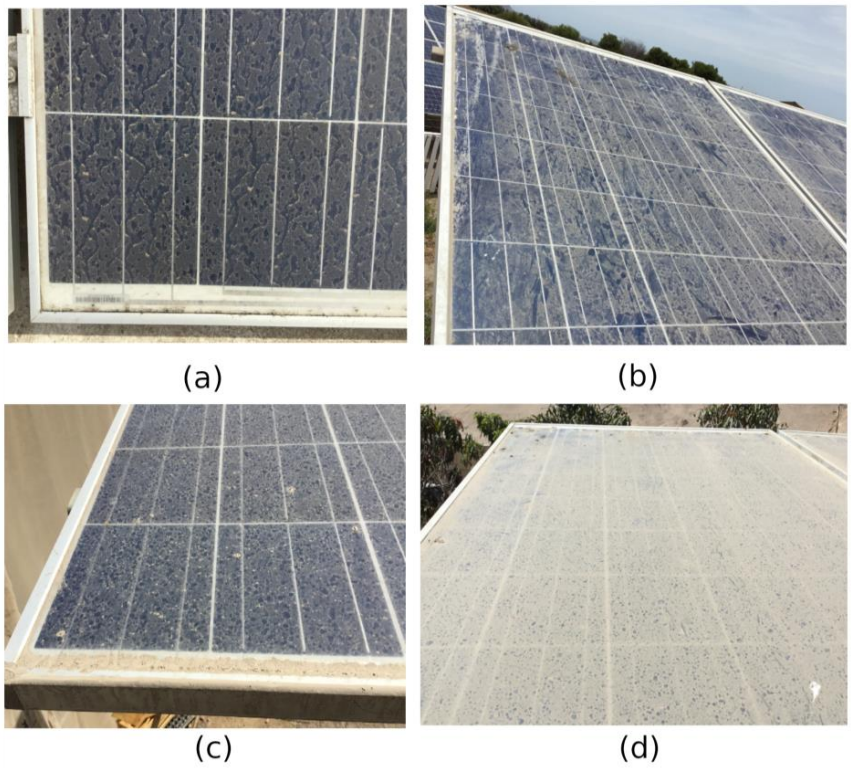

Figure 3: Different deposition patterns shown by heavily soiled modules according to their location: (a) coast, (b) coastal zone inside city and (c), (d) inner valley.

According to the classification of soiling by means of modules location, it was found that, in general, modules tend to show even temperature profiles (despite individual variations) with hotter cells at the bottom or centre of modules. Thermal images of modules according to their soiling type are shown in Figure 4 and the average operating temperature of modules belonging to each soiling type are shown in Table 3. As shown, average operating temperatures range from 37.9 to 47.9°C, despite individual cell temperature variations which will be detailed in next subsections.

Regarding to electrical measurements, deviations of V_{oc}, I_{sc} and P_{mpp} from their nominal values were calculated, given that all modules were operating for at least 2 years. As shown in Table 3, where the negative sign indicates reduction from nominal value, the most affected parameter of the I-V curve is the short circuit current, which ranges from 10 to 55% drop. On the other hand, voltage is also affected in a range between 3.5 to 4.7%. Both reductions, in V_{oc} and I_{sc}, contribute to P_{mpp} drops up to 63%.

Tab. 3: Average temperature [°C] and electrical parameters deviations [%] w/r to nominal values according to soiling types.

			Electrical parameters deviation [%]		
Zone	**Soiling pattern**	**Average temperature [°C]**	**V_{oc}**	**I_{sc}**	**P_{mpp}**
Coast	I	37.9	-3.7	-15.1	-18.5
Coastal city	II	38.4	-4.7	-10.1	-14.2
Inner valley	III	47.9	-3.5	-36.5	-19.1
	IV	42.5	-4.7	-55.3	-63.2

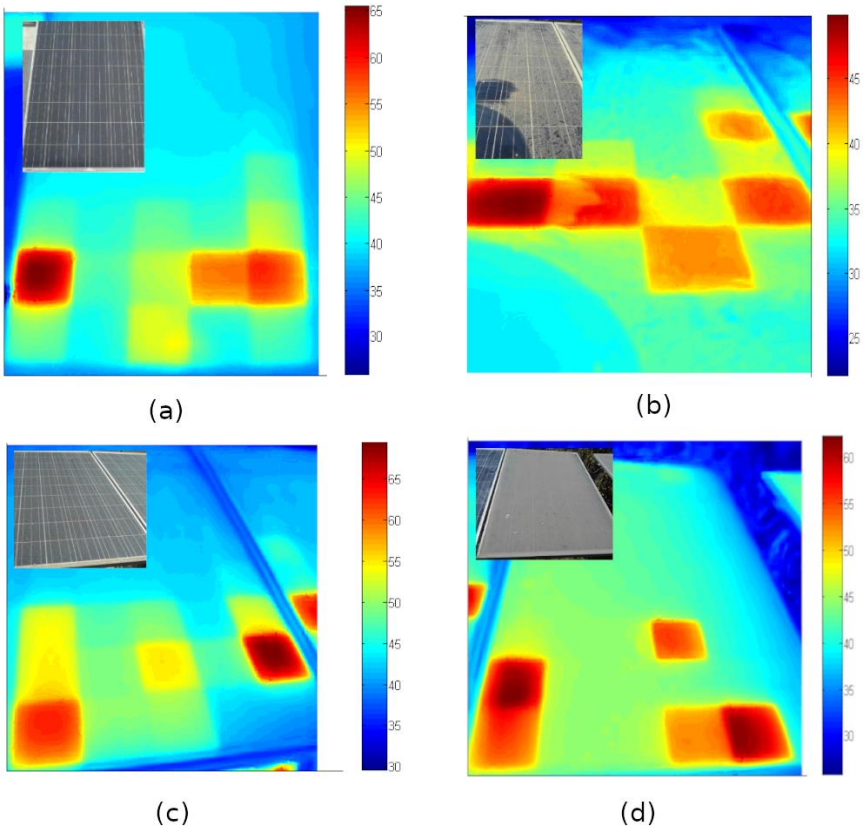

Figure 4: Thermal patterns of heavily soiled modules according to their soiling type: (a) coast, (b) coastal zone inside city and (c), (d) inner valley.

A special case was found in the inner valley with a soiling pattern type IV. Due to the extremely thick layer of soiling affecting those modules (see Figure 4d), their I-V characteristics show a severe decrease of both I_{sc} and V_{oc} parameters. In these 6 cases, two electrical measurements were performed: the first one with the module severely soiled and after the module was cleaned. First, it was observed that the short circuit current, which reductions ranged from 53.2 to 61.6% improved to a range between 2.8 to 12.9% with respect to the nominal value, therefore, losses due to this parameter were mainly due to the soiling layers. Voltage reductions were not as severe as in the case of the current, improvements for the open circuit voltage changed from 3.8 - 5.5% to 0.2 - 1.7%. On the other hand, temperature profiles show that module average temperatures were lower for the modules when they were dirty than after cleaned. Given that dirty modules generate a lot less current, then, thermalization losses also decrease, which explain why dirty modules are cooler. Temperature rising was between 2°C and 7°C after cleaning. Additionally, it was observed that in all modules the presence of strong hotspots (cells with temperatures higher than 20°C than the module average temperature) varied significantly from dirty to clean state. As shown in Figure 5, both, the plant shadow and the soiling layer, contribute to the reduction of electrical output, which is partially recovered after the module is cleaned. However, the hot cells shown in the dirty state are not the same than those in the clean state. Also, in the dirty case, the two hotspots are no hotter than 70°C, while in the clean case the hot cell at the corner reaches 99°C. A possible reason for this can be explained with the bypass diodes. In the dirty case the partially shaded string may be bypassed and after the cleaning and removal of the plant, the second string is bypassed (the cell in the 3rd string remains around 70°C). So it is probable that severe shunts remain covered by other external anomalies that cause activation of bypass. A similar behavior (electrical and thermal) was observed in the other 5 modules.

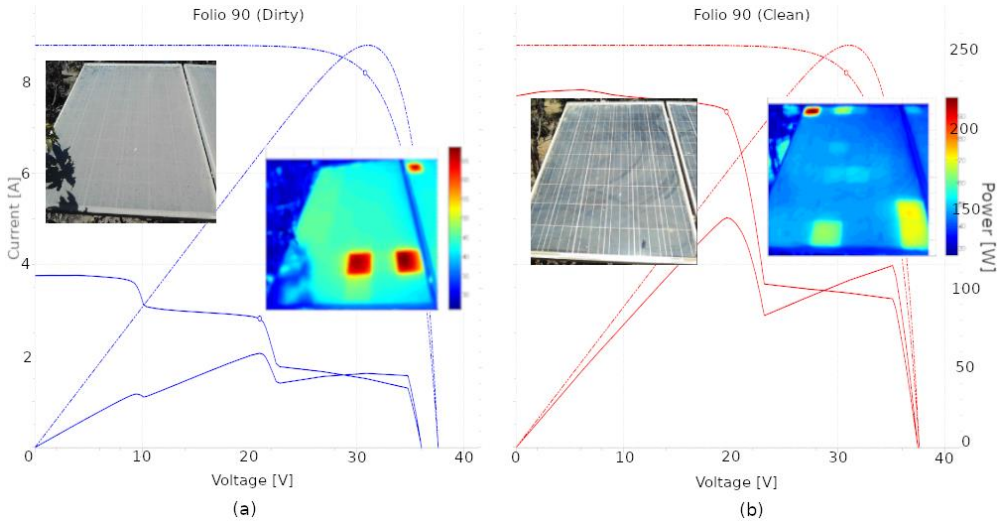

Figure 5: I-V/P-V characteristics, visual and thermal images of a module (a) heavily soiled and partially shaded, (b) after cleaning and cleared.

For lightly soiled modules, no specific soiling patterns were found, but those were mainly found in the city (zone B), inner valley (zone C) and inner coast (zone D). For those modules, given that fine layers of dust are not necessarily related to severe degradation or failures, no thermal pattern nor specific IV curve shapes were detected. However, in this case, reduction in the short circuit current was also observed but less severe than those of heavily soiled modules.

Being the most extended issue found in the analysed sample, soiling is also the easiest to revert, by simply cleaning the modules. In desert areas, a well-planned cleaning protocol can be a key to avoid further problems with PV modules. However, specialized training for small/domestic owners who may not be familiar to PV plants operation may assure a correct exploitation of them.

3.2. Hotspots

The analysis of hotspots regards to the analysis of thermal images, evaluating temperature variations detected from IR spectra measurements. As detection of hotspots is made by means of IR thermography and no direct correspondence with visual inspection or electrical measurements can be made in general (given the presence of multiple failure/degradation modes in each module), so underlaying mechanisms are difficult to establish with the available data. Despite de reason of heating (cell fracture, shading, short circuit, reverse bias operation, etc.) the cell temperature is determined also by the cell quality, which can be quantified by means of shunt resistance. However, this information is not provided by manufacturers, and is very difficult to measure in a fielded module.

Hotspots were found to be a very common issue affecting the evaluated modules, with almost 80% of them showing thermal anomalies between 10-20 °C and 56% above 20 °C with respect to the average operating temperature of modules. Most modules show multiple hotspots, in some cases following known thermal patterns (short circuited module, potential induced degradation, etc.). However, other thermal anomalies show correspondence with visual defects such as milky discoloration of the front glass and the presence of drops or shading. Also, a pair of modules show thermal patterns attributable to cracks and defective soldering, but to ascertain this diagnosis a more detailed visual inspection (or the use of additional tools like microscope or electroluminescence imaging) is needed. From the total sample universe, more than 50% of modules were operating with light hotspots, while in zones A and C more than 50% of modules were operating with strong hotspots.

However, further than the hotspot phenomenon itself, it was interesting to investigate the occurrence of this issue with respect to the module's manufacturer, deployment date and operating zone. For the analysis, hotspots temperature rising with respect to the average operating temperature were divided in five intervals: [10 – 20), [20 – 30), [30 – 40) and >50°C, named as I_i with i=1,…,5 respectively. Results are shown in Figure 6, where the % of modules (a-c-e) and the number of affected cells (b-d-f) with hotspots are plotted with respect to manufacturer (a-b), years of exposure (c-d) and operating zone (e-f). The number of affected modules is shown above the bars in each graphic.

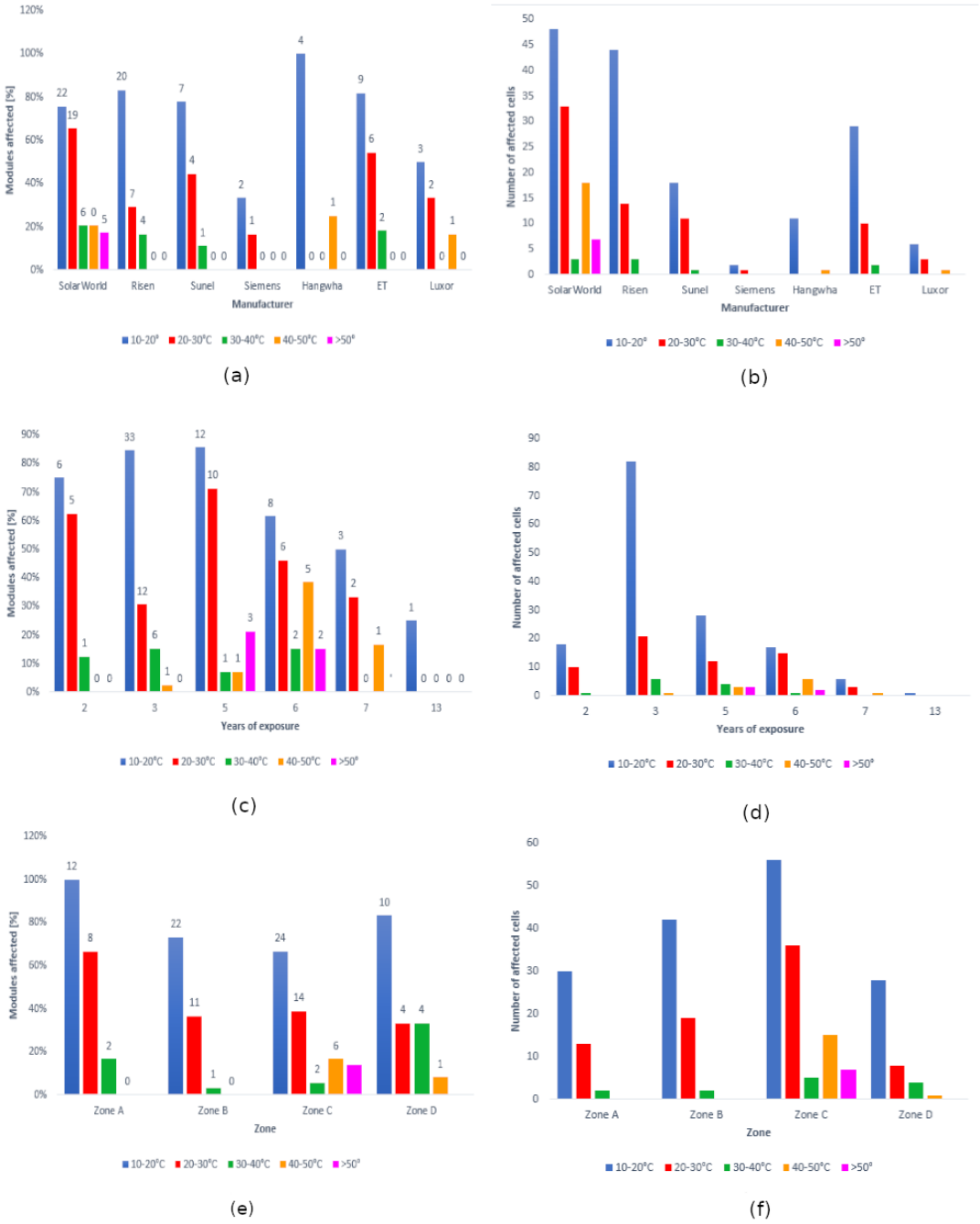

Figure 6: Hotspots occurrence divided in five temperature intervals, according to manufacturer, years of exposure and operating zone.

With a fast overview, it can be seen in a-b that only modules manufactured by SolarWorld show temperature differences above 50°C, with 17% of affected modules (5) and 7 affected cells. As shown in e-f, all these modules are in zone C, while the next higher temperature interval I_4 corresponds to modules of inner zones (coast and valley). Again, the higher number of hot cells correspond to those of zone C (SolarWorld), which indicates that the most severe heated cells are concentrated in a small number of modules, which also occur in zone B within the I_2 interval. The inverse situation occurs in zones A and D, where the total number of hot cells within the interval I_1 is distributed in (almost) all the modules of these zones. Within I_3, again SolarWorld shows the highest number of affected modules followed by Risen, but with only a few number of affected cells. The less affected modules were Siemens, Hangwha and Luxor, both in number of modules (6, 5, 6 respectively) and severity (no higher than I_3).

The highest cell temperature was 99°C, found in a SolarWorld module operating in zone C. Although this is not considered an extreme temperature (EVA encapsulant melts at temperatures higher than 150°C), cells operating under such thermal stress is not recommended, because other failure/degradation modes can be

induced/accelerated due to the large difference in thermal expansion coefficients between the semiconductor and metal components (He, et al., 2016). However, the small size of the sample universe does not assure statistical validity to this analysis.

3.3. Discoloration of front cover glass

Milky discoloration of the front glass is not a very documented topic, but it seems to obey a change in composition of the glass that prevents the passage of light to the cells. From the total sample, two modules were found to show extensive milky discoloration (ED), accompanied with a weathered surface appearance and a fine layer of soiling, while 6 other modules showed localized discoloration (LD), all at their bottom cells, added to a fine layer of soiling. All these modules are in the inner valley area (zone C) and at the time of inspection were operating for 6 and 7 years. Both these cases show alterations in their electrical parameters, mainly in I_{sc}. However, in some LD modules the measured voltage surpasses the nominal voltage, suggesting the presence of reverse biased cells, not enough to activate bypass. Also, a pronounced slope near the I_{sc} is observed, suggesting a decreased shunt resistance. This is reinforced by the thermal images, which show severely heated cells in the areas of LD, as shown in Figure 7, reaching temperatures between 80 and 94°C.

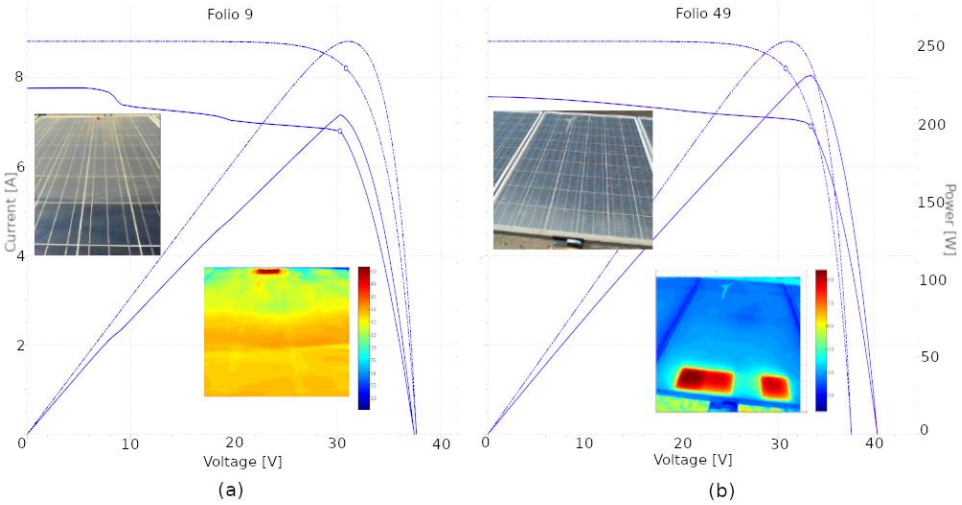

Figure 7: I-V/P-V characteristics, visual and thermal images of modules with milky discoloration of the front cover glass (a) extensive, (b) localized in the bottom cells.

While for a precise diagnosis of the underlying mechanisms that may be causing this issue, data provided from visual inspection, electrical measurements and thermal images suggest that interactions between the front glass and the environment are affecting the glass features. Despite the aridity that characterizes these locations, weathering was also observed, and thermal images show that the cells affected by discoloration are being forced to currents higher than they can deliver, thus, leading to severe heating. For further study, it would be interesting to research elemental interactions (changes in structural composition, optoelectronic features) of environmental particles surrounding modules and the front glass, considering that this last may vary from one manufacturer to another.

3.4. Partial shading

Partially shaded cells were found, in all zones, in three ways: modules shaded by plants/trees, cells with mud or bird drops, and cells with localized dust deposition. As shown in Figure 8, a comparison between visual inspection and thermal profiles show that in the case of a localized dust deposition (a) the hottest area of the cell, although near, is not completely coincident with the shaded area. The temperature difference between the hottest point of the cell and the rest of the module is very high (dT = 40.6°C), which can be an indicative of other issues (shunts, for example). For other partially shaded cells, severe heating was neither found. As shown in Figure 8b-c, temperature differences of shaded areas and the rest of the cells are between 3 - 6°C while these differences with respect to the rest of the module do never surpass 7°C. All these modules were found to be operating within zones A and B (coast and city) for which the presence of birds and moisture are more common than those of inner zones.

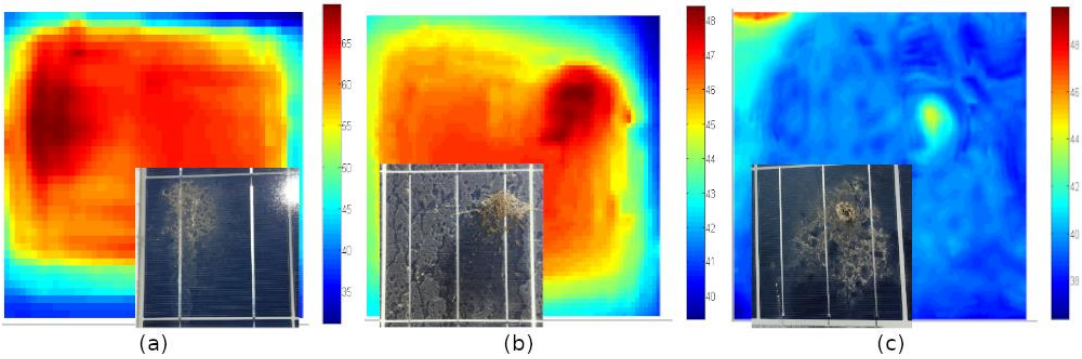

Figure 8: Visual inspection and thermal profiles of partially shaded cells by (a) localized dust deposition, (b) mud drop and (c) bird drop.

Regarding to modules partially shaded by trees or plants, found in zone C, where the land sharing between PV facilities and other activities (mainly agricultural) is very common, the following was found. As shown in Figure 9, the shaded area comprises the upper left cells of the module, which thermal profile shows a notable change in temperature within the most shaded cells. It can be noted that shaded areas are characterized by cooler temperatures (with respect to the rest of the module), while non-shaded areas within the affected cells show a temperature rising up to 52°C. The I-V/P-V characteristics shows a notable current mismatch between one string and the rest of the module, probably due to the limited generation of the shaded string. However, the module also shows a strong hotspot non-correlated to visible anomalies and a layer of soiling on its surface. Therefore, the electrical behaviour of the module cannot be attributable entirely to the shading effect.

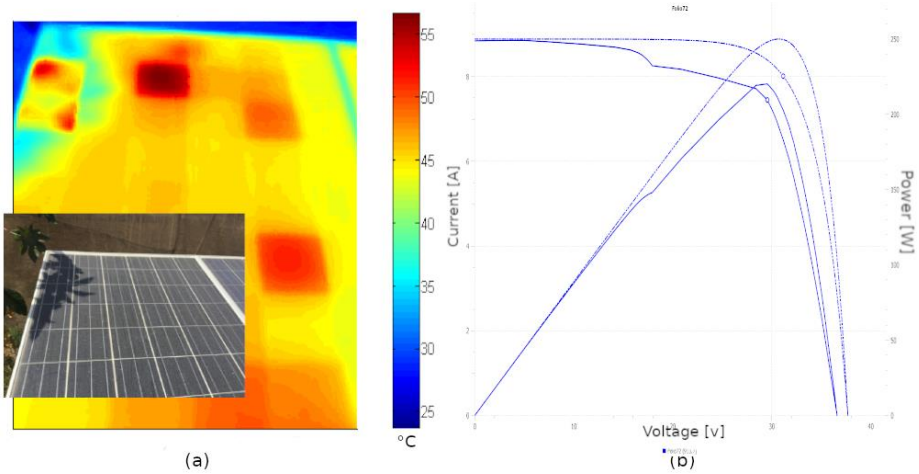

Figure 9: (a) Visual inspection, and thermal profiles and (b) I-V curve of a partially shaded module due to the presence of a tree.

3.5. Other anomalies

Other anomalies found in the inspected sample universe are briefly described in this section, suggested by simple visual inspection, thermal patterns or I-V characteristics. However, either this information could not be matched with other measurements (electrical, thermal or visual) or it was found in a single species. Delamination of the EVA encapsulant, shown in Figure 9b, was found in 4 modules. On three of them, delamination appears to be extended through the entire surface but showing clear paths (like snail trails). The remaining of the module shows very localized bubble-shaped delamination around busbars. Electrical measurements in the three extensively delaminated modules were made under bad irradiance conditions ($G < 600$ W/m^2), and the other module evidenced action of the bypass diode, so these measurements are not reliable enough to conclude the effects of delamination. Thermal images do not show correspondence between the delaminated areas and thermal anomalies, although they show several cells under thermal stress between 37 and 55°C. However, these modules were deployed only three years before the field test campaign was performed. Therefore, it is possible that delamination as a degradation mode is present in its very early stages and do not affect yet the passage of light towards the cells.

A possible fractured cell and faulty soldering were suggested by characteristic thermal patterns. In the first one, the temperature distribution across the affected cell shows an uneven shape, with a well-defined temperature change of about 3°C from the lower right corner to the rest of the cell, which appears to be hotter. It is usual that cell fragments get isolated from the rest of the cell (thus not contributing to the overall current) decreasing their temperature. However, current mismatch or a visible fracture were not detected in the

electrical measurements or the visual inspection, so further analysis is required in this case. Faulty soldering can be also detected by an uneven temperature distribution, as shown in Figure 9a, in this case one half of the cell appears hotter than the other half. In this case, the thermal abnormality found corresponds with a slightly increase of the series resistance in the I-V curve.

The last interesting case was a module with a thermal pattern and I-V characteristics of Potential Induced Degradation (PID). In domestic PV facilities, it is common to find defective, or even absent grounding systems, which may favour the appearance of PID issues. In the case of the Atacama Desert, it is more common to find modules suffering from PID in the coastal region. This corrosive salty environment promotes leakage currents between the cell, front glass and aluminium frame. As shown in Figure 9c, this module shows hotter cells mostly at its bottom and mid regions, and upper region near the frame. The temperature differences are roughly 5°C from the PID affected zones in comparison to the rest of the module, with one warmer cell at the bottom (near 45°C). Electrical measurements show degradation of V_{oc} and rounding of the knee, at the $P_{mpp.}$

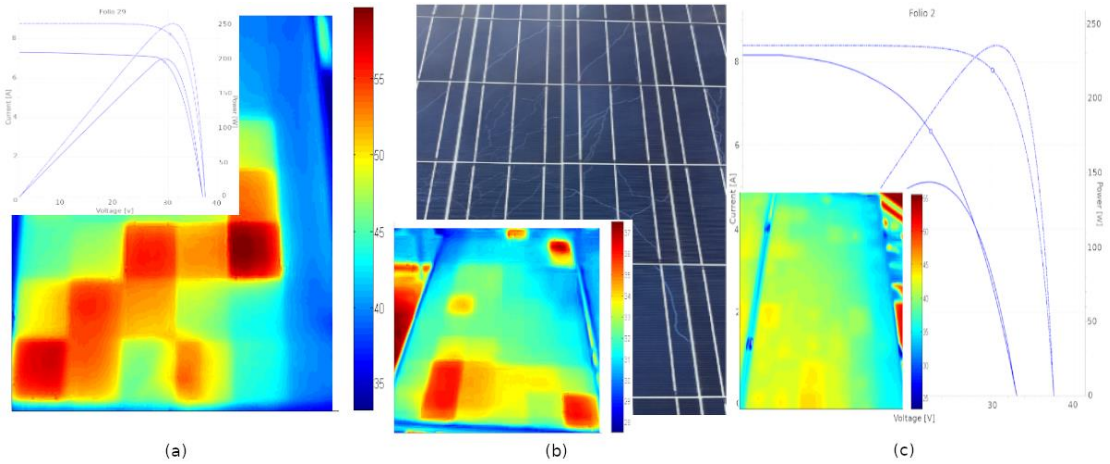

Figure 9: Thermal and visual detection of (a) possible faulty soldering, (b) slight delamination and (c) PID.

4. Conclusions

An analysis was performed on failure and degradation modes found in 95 modules deployed and operating in the Atacama Desert, Chile. Four different zones were delimitated according to each of their geographic features: coast (high humidity and coastal wind), inner coast (less humidity, more dust), city (varied pollutants) and inner valley (high aridity and dust, low humidity). As a result, eight different anomalies were detected by means of three inspection tools: visual information, thermal images, and electrical measurements of the I-V characteristics. The most extended issue found was soiling, in different deposition degrees depending on their location, being the inner valley the most affected zone. Hotspots were found in more than 50% of the inspected modules, with temperatures ranging from 20 to 50°C. The highest cell temperature found was around 100°C, which is not necessarily hazardous for module operation or system safety. However, it generates thermal stress that can induce/accelerate degradation of cells or encapsulant materials. The hotspots entailing the most severe issues were found in two sets manufactured by SolarWorld, which were located in the inner valley of the region under research. One of these sets was affected by a milky discoloration on the front glass, located at the bottom of the modules. All the hotspots correspond to the discolored area of the glass, which may indicate that chemical changes occur by action of external variables (such as environmental soiling particles, moisture, UV degradation, etc.). The other set was affected by a heavy soiling layer. However, after cleaning the modules, no relationship between this phenomenon and hotspots was observed. On the other hand, soiling phenomena were found to affect more the I-V characteristics than thermal distribution. Other anomalies such as partial shading, delamination of the EVA encapsulant, faulty soldering, and cell fracture could be identified and described with varying accuracy. Partial shading was found to occur due to several factors depending on the location of the modules: massive shadows projected by trees/plants, bird drops, mud drops or localized soiling deposition due to uneven module cleaning and, in all cases, temperature differences within the shaded areas were not higher than 7°C. Also, slight changes on the I-V curve were observed, such as increased slope or current mismatch steps. Delamination of the EVA encapsulant was found only in 4.2% of the total sample universe. No severe cases were identified as visual inspection revealed that snail-trail-shaped delaminated areas (not extended through large areas of the modules), and the thermal patterns of the modules affected did

not show a relevant correlation between delaminated areas and temperature anomalies. Faulty soldering and fractured cells were inferred by a characteristic thermal signature. Such signature shows, in the first case, that one half of the affected cell was hotter than the other half and, in the second case, that a small well-defined area of the cell was colder than the rest of the cell. As for the faulty soldering, a slight increase in the series resistance was observed in the I-V curve. However, more inspection tools are needed to achieve a complete diagnosis. Finally, one case of PID was detected by means of IR images and I-V measurements. As for failure/degradation mechanisms, some of them can be attributable to natural environmental conditions of the Atacama Desert, such as UV radiation, presence of moisture (despite the characteristic aridity of the desert), wide thermal cycling, among others. However, more specific research is needed for an accurate diagnosis. Others, such as PID, may be attributable to defective/non-existent system grounding. In the case of soling, simple strategies such as training, or design of cleaning protocols for domestic owners can improve the situation. An interesting relationship between external desert variables and the front glass of some modules was identified, thus, further research about the effect of certain soiling composites, as found in (Douglas, et al., 2017), and the soda-lime glass surface is recommended. However, simultaneous occurrence of multiple failure/degradation modes difficult the identification of corresponding failure/degradation mechanisms. This work constitutes a first effort to characterize small-scale domestic PV solutions in extreme Chilean desert conditions. It may be used as a basis for a systematic performance assessment of community-level solar solutions in Latin America.

5. Acknowledgments

This research was supported by the FONDAP/CONICYT Nº 15110019.

6. References

Angèle, R., Pierre, V., Wilfried, v. S. & Alexandre, F., 2016. Reliability and Durability of PV. En: *Photovoltaic Solar Energy: From Fundamentals to Applications*, Wiley, pp. 492-494.

Buerhop, C. et al., 2012. Reliability of IR-imaging of PV plants under operating conditions. *Solar Energy Materials and Solar Cells*, Volumen 107, pp. 154-164.

Devoto, M. I., 2018. *Solar module characterization via visual inspection in the field, I-V curve and thermal image analysis.* Santiago de Chile, Universidad de Chile.

Douglas, O. et al., 2017. Characterization of soiling on PV modules in the Atacama Desert. *Energy Procedia*, Volumen 124, pp. 547-553.

Eder, G. C. et al., 2018. Climate specific accelerated ageing tests and evaluation of ageing induced electrical, physical, and chemical changes. *Progress in Photovoltaics*, pp. 1-16.

Felder, T. et al, 2015. *Development of backsheet tests and measurements to improve correlation of accelerated exposures to fielded modules.* San Diego, California, Society of Photo-Optical Instrumentation Engineers (SPIE).

Ferrada, P., Rabanal, J., Marzo, A. & Cabrera, E., 2015. AtaMo: PV meets the high potential of the Atacama Desert. *PV Tech Power*, Volumen 5, p. 55.

Guiheneuf, V., Delaleux, F., Riou, O. & Logerais, P.-O., 2016. *Investigation of Damp Heat aging on soda-lime glass for photovoltaic applications.* Munich, Germany, s.n.

He, W., Ao, W., Hong, Y. & Dengyuan, S., 2016. Analysis of the Thermal Stress for Combined Electrode of Soldered Crystalline Silicon Solar Cells under Temperature Field. *International Journal of Photoenergy*, p. 7.

Jordan, D. C. et al. 2017. Photovoltaic failure and degradation modes. *Progress in Photovoltaics*, 25(4).

Köntges, M., Kurtz, S., Packard, C. & Jahn, U., 2014. *Review of Failures of Photovoltaic Modules*, St. Ursen, Zwitzerland: IEA-PVPS.

Mazumder, M. K., Horenstein, M. N., Heiling, C. & Stark, J., Photovoltaic Specialist Conference (PVSC). *Environmental Degradation of the Optical Surface of PV Modules and Solar Mirrors by Soiling and High RH and Mitigation Methods for Minimizing Energy Yield Losses.* New Orleans, LA, IEEE.

Menoufi, K., 2017. Dust Accumulation on the Surface of Photovoltaic Panels: Introducing the Photovoltaic Soiling Index (PVSI). *Sustainability*, 9(6).

Ministerio de Energía., 2014. *Energía 2050*. [Online]
Available at: http://www.energia.gob.cl/sites/default/files/energia_2050_-_politica_energetica_de_chile.pdf.

Rondanelli, R., Molina, A. & Mark, F., 2015. The Atacama Surface Solar Maximum. *Bulletin of the American Meteorological Society*, 96(3), pp. 405-418.

Sai Tatapudi, J. K. G. T., 2018. *A novel climate-specific field accelerated testing of PV modules.* San Diego, California, USA.

Subramaniyan, A. B., Pan, R., Kuitche, J. & TamizhMani, G., 2018. *Prediction of Acceleration Factor for Accelerated Testing of Photovoltaic Modules Installed Around the World.* Reno, NV, USA, IEEE.

Trang, et al., 2016. Effects of UV on power degradation of photovoltaic modules in combined acceleration tests. *Japanese Journal of Applied Physics*, 55(5).